Characterization of suprathermal electron population in He dc glow discharges by optical emission and probe diagnostics

A B Mart´ın-Rojo[1,2], E Oyarzabal[1,3] and F L Tabarés[1]

[1] Asociacio´n EURATOM-CIEMAT, Ave. Complutense 22, 28040 Madrid, Spain
[2] UC3M. Madrid, 126. 28903 Getafe, Madrid, Spain
[3] U.N.E.D. Ciudad Universitaria, S/N, 28040, Madrid, Spain

E-mail: paco.tabares@ciemat.es

Abstract

Evidence of the strong contribution of electrons with energies up to the cathode fall potential was found in low-pressure He dc glow discharge plasmas (3–8 mTorr), in agreement with expectations from the estimates of the mean free path of electron–neutral inelastic collisions. A simple gridded probe, of the retarding field analyzer type, was applied to the characterization of the full electron energy distribution function (EEDF) in He plasmas with significant contribution from suprathermal electrons (up to 3.5%). The inferred EEDFs were cross-checked with results from the He line ratio diagnostic and good agreement was found at several values of pressure and plasma current.

(Some figures may appear in colour only in the online journal)

1. Introduction

In a dc glow discharge, the main role of the secondary electrons produced at the cathode by ion impact is to sustain the plasma by ionizing collisions with neutrals [1]. These electrons are born with modest energies but they are quickly accelerated by the local electric field developed at the cathode fall region near the walls. Depending on the local field strength and neutral pressure, some of these electrons cannot be accommodated into the plasma bulk and they can reach the anode with a significant fraction of their initial energy, thus leading to the formation of a suprathermal energy tail in the electron energy distribution function (EEDF) of the plasma. From the power balance point of view, non-collisional electron components represent not only a waste of energy but also a source of overheating of some parts of the reactor, particularly the anode. In fusion energy plasmas, the so-called runaway electrons are indeed a potential driver of material damage as they develop hot spots in the components intercepting them [2] with deleterious consequences.

Several techniques have been devoted to the quantification of such energetic tails in the EEDF with varying success. The analysis of the I–V characteristics of simple Langmuir probes near the floating potential represents the simplest approach [3]. However, the concentration of electrons with energies in the suprathermal range is typically in the order of <1%, so that the intrinsic noise associated with the current measurement sets a rather poor limit for this application. Retarding field analyzers have also been successfully applied to this end. However, only energies below ∼50 eV have been reported by this technique [4]. For higher energies, secondary electron emission of the electrodes used in all kinds of probes becomes a serious constraint. Optical methods, which do not suffer from this problem, offer an alternative diagnostic. So, for example, an optical probe based on the excitation of neutrals in a restricted volume, on which only electrons with energies over a threshold value set by a biased grid were allowed, was developed by Sugai *et al* [5]. The functional dependence of the emitted light was used for the reconstruction of the EEDF. More frequently, the ratio between the line emission from two excited states showing different dependences on electron energy was applied for the estimation of an effective excitation temperature. This temperature is strongly dominated by the energetic components of the distribution due to the exponential rise of the corresponding cross-sections with energy. This is the so-called line ratio diagnostic, also in wide use in fusion plasmas for the case of He atoms [6].

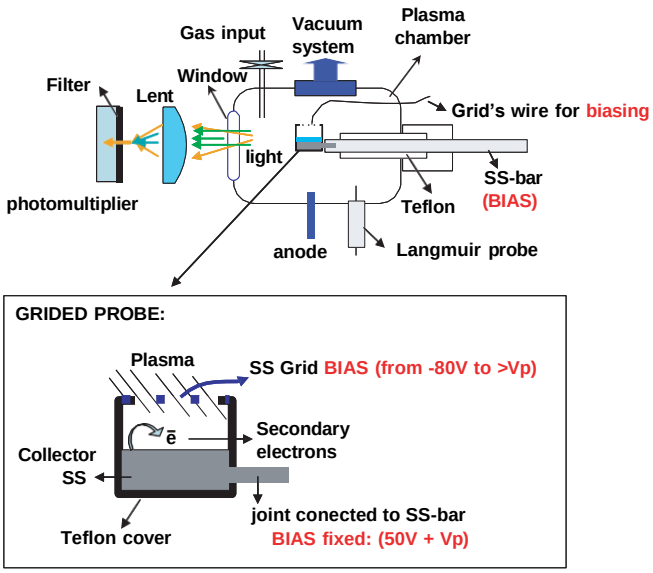

Figure 1. Experimental set-up.

In this work, we address the characterization of the full EEDF in a low-pressure, dc glow discharge of He. Two different diagnostics have been used for the characterization of the EEDF, a gridded probe and the line ratio of two He lines corresponding to a singlet and a triplet excited level, respectively. The results of the gridded probe show a bi-Maxwellian type of electron distribution for all the studied cases. The evolution of the bi-Maxwellian distribution with pressure and source current is also addressed.

2. Experimental set-up

The present experiments are carried out in the set-up shown in figure 1. The plasma reactor consists of a grounded stainless-steel cylindrical vessel (35 cm diameter, 50 cm length) acting as the cathode and the anode placed on a side of the chamber [7]. In this study, the characteristics of the dc glow discharges produced in the main chamber are addressed. In order to measure them, a simple gridded probe, used as a retarding field analyzer, is mounted on a manipulator to obtain the electron energy distribution of the plasma for the different conditions under study. It consists of a grid which is biased from −80 V to a potential higher than the plasma potential and a collector which is biased to a sufficiently high positive voltage to repel the ion current passing through the grid and to retain the secondary emission electrons that are created in the collector. In this manner, the current collected at the different voltages applied to the grid directly represents the electron current arriving at the grid at each studied voltage. A similar probe was used by Blackwell and Chen [8] in a radio-frequency (RF) helicon plasma. A grid spacing of 0.5 mm (smaller than the Debye length for all the studied conditions) is used in order to block any plasma from reaching the collector while a distance of 2 mm between the grid and the collector (much less than any electron collision length) ensures that the electrons which pass through the grid reach the collector unimpeded, and that no ionizing collisions occur in the region between the two [8].

Table 1. Main parameters (from Langmuir probe analysis) of the studied plasma discharges.

Current (mA)	Pressure (mTorr)	V_p (V)	n_e (cm^{-3})	T_e (eV)
100	8	231	4×10^8	9.6
100	5	246	1.7×10^8	8.8
100	3	330	1.5×10^8	10.4
300	8	226	9.4×10^8	7.2
300	5	254	5.5×10^8	9.3
300	3	357	1.03×10^9	8.9
500	8	223	6.3×10^8	6.5
500	5	263	8.6×10^8	7
500	3	366	No data	No data

Furthermore, a photomultiplier/interference filter (filterscope) system is used to detect the He 728 nm and 706 nm emission lines from a side window in order to measure the effective temperature of the plasma by the well-known line ratio method [9]. The system was calibrated using a reference lamp (AVANTES, HL-2000-CAL). In addition to these specialized diagnostics, a single W Langmuir probe (0.4 mm diameter, 6 mm length) directly inserted into the He plasma is used for the recording of the microscopic parameters, electron density (n_e) and temperature (T_e), and plasma potential (V_p) of the main discharge. No influence of the biasing of the gridded probe on the recorded signals at the Langmuir probe was detected within the natural noise of the measurements, so it is assumed that non-perturbative conditions for the gridded probe operation prevailed.

The different plasma discharges studied for the different plasma currents and their main parameters are shown in table 1. The reader should bear in mind that, as has been explained previously, the effect of the suprathermal tail in the Langmuir probe can lead to significant errors in the results of the same, which is precisely the reason why other characterization techniques are needed to fully address the kind of electron energy distributions observed in this work. As can be seen, these are low-pressure discharges with a high plasma potential, a very favorable scenario for the existence of suprathermal electrons.

3. Results

3.1. Dc glow discharge characterization: He (728 nm)/(706 nm) line emission

Under the simplest possible scenario, the emission intensity of excited atoms (X^*) in a plasma is given by

$$I_{X^*} = A(\sigma v)_{ex}[X]n_e, \quad (1)$$

where $(\sigma v)_{ex}$ accounts for the excitation rate from the ground state of X to the particular electronically excited state whose emission is recorded, n_e is the electron density of the plasma, $[X]$ is the density of the ground state atoms of X, and A is a constant accounting for the probability of decay to the particular level with respect to all possible transitions, the so-called branching ratio, as well as for the sensitivity of the detection system, which must be calibrated with respect to a

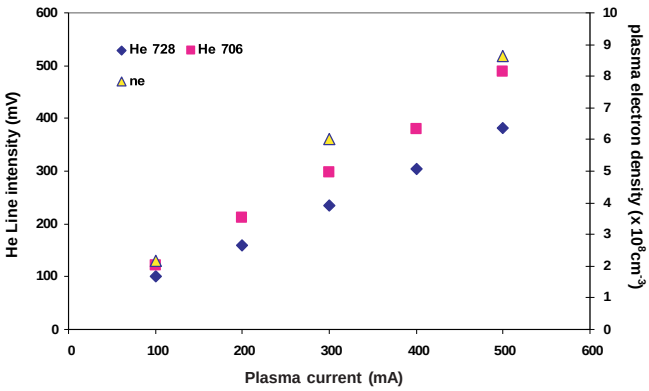

Figure 2. He 728 nm and He 706 nm line intensities and plasma density linear functionality with plasma current for the case of constant pressure (5 mTorr).

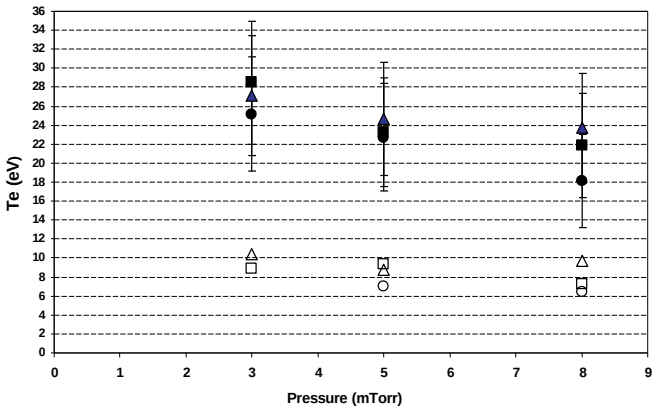

Figure 3. Comparison of the bulk T_e from Langmuir probe (hollow symbols), and the effective T_e from (728 nm)/(706 nm) He line experimental ratio (filled symbols) at several pressures and source currents (•.6 100 mA; ■ ▫ 300 mA; ○ • 500 mA).

known source. The excitation cross-section, σ_{ex}, is strongly dependent on the electron energy for values near the excitation threshold, around 20 eV for He atoms, and it must be integrated over the actual EEDF, in order to get the effective excitation rate. If two lines showing different functional dependences on electron energy are simultaneously monitored, it is possible to obtain an effective electron temperature by recording their intensity ratio with a simple interference filter/photomultiplier arrangement (filterscope). This is known as the line ratio method, of ample application in cold plasma diagnostics.

In the case of He, a different behavior of the excitation cross-sections for the singlet and triplet manifolds exists. This opens the possibility of non-invasive diagnostics for the electron temperature by choosing the suitable lines emitted by the plasma. In this work, the ratio of the (728 nm)/(706 nm) He line emission, corresponding to electronic excitation to the 3^1S and 3^3S levels, respectively, is used to obtain the value of the effective electron temperature of the plasma for the different conditions addressed here. Since the electron densities of our plasmas are under 10^{10} cm^{-3} for all cases, the steady-state corona model for the evaluation of the density of the excited states can be used with reasonable accuracy [10]. Helium electron impact excitation cross-sections from the ground state are taken from a database [11] and the excitation rate coefficients are calculated by assuming a Maxwellian electron velocity distribution. The electron temperature is then obtained by measuring the intensity ratio of He transitions from the plasma. By this procedure, however, only an 'effective temperature' defined as the temperature of the single Maxwellian distribution of electrons that would produce the same line intensity ratio is obtained.

The proportionality of the emission intensity with electron density predicted by equation (2) is tested under the current and pressure values used in this work. Examples of linear functionality of the line intensity with plasma current and density at constant pressure are given in figure 2.

Figure 3 shows the resulting effective temperatures for the different pressure and discharge current values under study. Higher temperatures are deduced for lower pressures and higher plasma potentials. The bulk electron temperature for each case obtained from the analysis of the single Langmuir probe [12] is also shown in figure 3. The effective temperature is clearly higher than that deduced from the I –V probe characteristics for all cases, thus implying the existence of a suprathermal electron population. These kinds of suprathermal populations have previously been reported in glow discharges [13–17]. Several possible sources for their generation have been put forward. Penning processes, together with other atomic processes, have been reported as a possible source of high-energy electrons in a glow discharge plasma [18] although at much lower energies than those found in this work. In our system, with energies up to 300 eV, they must come from the secondary emission electrons from the discharge chamber walls that are accelerated to the plasma potential in the sheath and do not get thermalized by the plasma collisions. For lower pressures the population is larger because the energy loss of these particles due to collisions with neutrals is lower.

3.2. Dc glow discharge characterization: EEDF from the retarding field analyzer

The use of a single, planar Langmuir probe to obtain the EEDF from the differentiation of the I –V curve [3] is strongly discouraged under the presence of high-energy suprathermal electrons with energies of about 300 eV, as found in our plasma, because the secondary electron emission from the probe itself is not negligible. Even though this population is very small with respect to the thermalized population (less than 3.5%), due to their high energies their current can be sufficiently high to generate a significant secondary electron component at the probe hard to compensate for. According to [19] electrons approaching a sufficiently large planar disk probe oriented perpendicular to the z-axis have only their z-component of velocity changed by the probe bias potential, and the one-dimensional electron distribution function can be obtained from the I–V characteristics with the following equation:

$$\mathrm{EEDF}_1(-q<P) = \frac{m}{q^2 A}\frac{\mathrm{d}I(<P)}{\mathrm{d}<P}, \qquad (2)$$

where q is the absolute value of the charge, A is the probe area, m is the electron mass, I is the measured current and $<P$ is the bias potential measured relative to the plasma potential.

For probe data that have been digitized, derivatives are most easily obtained using finite differences. The projected distribution $EEDF_1$ is

$$\mathrm{EEDF}_1(-q<P_{k-1/2}) = \frac{m}{q^2 A}\left(\frac{I_k - I_{k-1}}{<P_k - <P_{k-1}}\right), \qquad (3)$$

where, for second-order accuracy, the potential at the midpoint of the interval $<P_{k-1/2} = 0.5\,(<P_k + <P_{k-1})$ is used.

Figure 4 shows the results for the mono-dimensional energy distributions measured in this manner with the gridded probe. In all the cases, the measured EEDFs are well fitted to a bi-Maxwellian distribution, which represents two fractions of the electron population: highly energetic electrons or '*hot*' electrons (suprathermal electrons) and electrons with less energy or '*cold*' (bulk) electrons, expressed in the form

$$\mathrm{EEDF}_1(E) = (1 - f_{\mathrm{hot}}) \times \sqrt{T_{\mathrm{cold}}} \times \exp(-E/T_{\mathrm{cold}}) + f_{\mathrm{hot}} \times \sqrt{T_{\mathrm{hot}}} \times \exp(-E/T_{\mathrm{hot}}), \qquad (4)$$

where T_{hot} and T_{cold} correspond to the temperature (eV) of the *hot* electrons and *cold* electrons, respectively, and f_{hot} is the suprathermal electron fraction.

The fitted bi-Maxwellian EEDFs for the different studied pressures and discharge currents are also shown in figure 4 and the fitting parameters are shown in table 2. As was observed from the He line ratio method, the suprathermal electron population increases with decreasing pressure and increasing plasma potential.

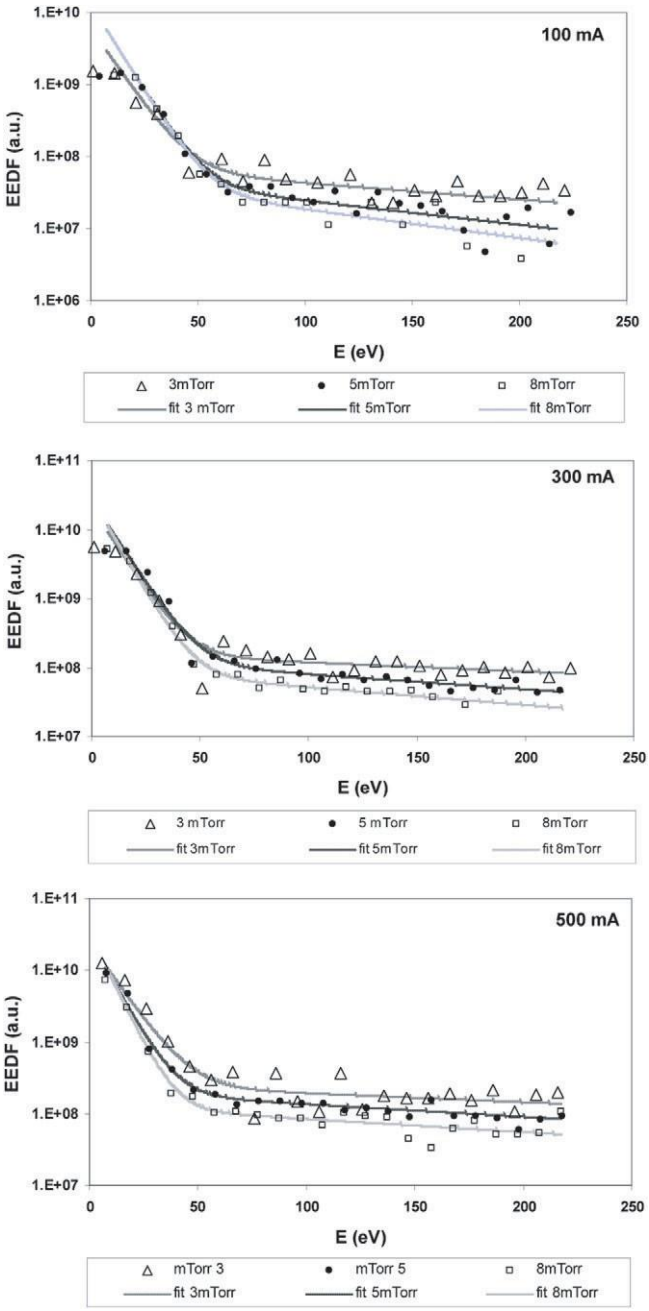

Figure 4. Mono-dimensional electron energy distributions measured with the gridded probe and fitted bi-Maxwellian distributions for the different studied pressures and plasma currents.

4. Discussion

4.1. Comparative results from the OES and probe data

In order to compare the two different methods used to characterize the electron distribution in our experiments, the theoretical line ratios that would be obtained from the EEDF provided from the gridded probe results are calculated from equation (2) for the case of the 3^1S and 3^3S levels, respectively. For each studied case $(\sigma v)_{\mathrm{ex}}$ is obtained from

$$(\sigma v)_{\mathrm{ex}} = \int \mathrm{EEDF}(E)\sigma_{\mathrm{ex}}(E)v\,\mathrm{d}E. \qquad (5)$$

Figure 5 shows the results of the ratios obtained in this manner and the experimental ratios shown before. The ratios from both methods seem to be in agreement with respect to the evolution with pressure, although the values for the case of He experimental ratio seem to be systematically higher. The errors due to the scattering of the data in the fitting of the EEDF and in the measurement of the He line ratios (also shown in figure 5) are not sufficiently large as to account for this difference. Nevertheless, the factor relating the ratios deduced from both diagnostics is fairly constant, suggesting a systematic effect.

There are different possibilities that could explain this disagreement. In the first place, the assumptions that are made to obtain the ratios from equation (2) that are usually applied to single Maxwellian electron distributions may not be valid for this case. This effect has been reported in previous works whenever a high-energy tail exists in the EEDF, and an agreement of a factor of two in the reconstructed microscopic parameters was taken as reasonable given the intrinsic errors of each technique [9]. It must also be kept in mind that the line ratio method is an integral one, while rather local values of the EEDF are obtained by the probe. For electrons produced at the reactor walls by ion impact and accelerated in the cathode sheath, a progressive slowing down by inelastic collisions with the plasma neutrals takes place, so that a profile with decaying ratios would be obtained by local measurements. This sort

Table 2. Fitting parameters of the electron bi-Maxwellian energy distribution function (see equation (4)).

Current (mA)	Pressure (mTorr)	T_{cold} (eV)	T_{hot} (eV)	f_{hot}
100	8	9	70	0.015
100	5	9	75	0.02
100	3	10	110	0.035
300	8	8	110	0.01
300	5	9	120	0.018
300	3	9	185	0.022
500	8	6	120	0.008
500	5	7	140	0.011
500	3	9	200	0.016

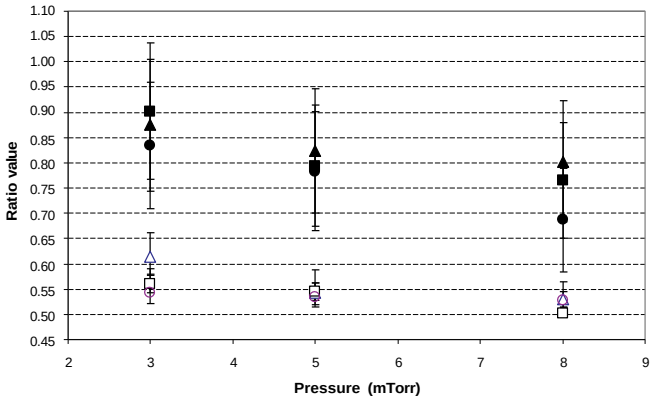

Figure 5. Comparison of theoretical ratio calculated with the EEDF obtained from the gridded probe measurements (open symbols) and the experimental ratio from measured He line intensities [(728 nm)/(706 nm)] (filled symbols) for the different studied pressures and plasma currents (•.6 100 mA; ■ ◘ 300 mA; ○ • 500 mA).

of profile was indeed seen, although only qualitatively, when sweeping the optical diagnostic across the plasma radius. Even if the optical system is focused to the same point where the probe is located, integration across the longitudinal component of the reactor cannot be avoided. Finally, a possible underestimation of the suprathermal population due to sheath edge effects in the gridded probe method could add up to the difference in the ratios.

4.2. EEDF evolution with pressure and current

For all the studied currents, the suprathermal electron fraction (f_{hot}) increases with decreasing neutral pressure. This effect has been reported previously in several studies for the case of capacitively coupled RF discharges [13–15] and dc glow discharges [13, 16, 17].

In some cases [15] an evolution from a Maxwellian to a bi-Maxwellian distribution was measured as the pressure of the system was decreased. A larger suprathermal population is indeed expected at the plasma center for lower pressures due to lower rate of inelastic collisions with neutrals within the plasma radius. The cross-sections for such collisions, including only ground state He, are shown in figure 6 for reference [20].

At the cathode (reactor wall) the number of secondary electrons produced by ion impact, and prone to acceleration in the sheath, would depend only on the energy of the impacting ions and their flux. The flux of secondary electrons released from the wall and accelerated by the sheath would be expressed as

$$r_{e\text{-hot}} = (I_p/A \cdot q) \cdot \mathrm{SEE} \qquad (6)$$

with I_p being the plasma intensity, A the nominal area of the reactor, q the elementary charge of the electron and SEE the secondary electron emission coefficient.

If these electrons are accelerated to the cathode fall potential, then their density (n_{ehot}) near the wall would be

$$n_{ehot} = 4 \cdot r_{ehot}/v_{e\text{-}}, \qquad (7)$$

where $v_{e\text{-}}$ is the electron thermal velocity.

For example, in our system, for $I_p = 100$ mA and $P = 5$ mTorr, the cathode fall potential is 246 eV (table 1), so $\bar{v}_{e\text{-}} = (kT_e/m_e)^{1/2} = 6.5 \times 10^8$ cm s^{-1}, and the recorded electron density is $n_e \sim 2 \times 10^8$ cm^{-3} (figure 2). Assuming a SEE of 0.3 e$^-$/He ion [21] and $A = 5 \times 10^3$ cm^2, a $r_{e\text{-hot}} = 3.7 \times 10^{13}$ e$^-$ cm^{-2} s^{-1} is obtained, so $n_{ehot} = 2.3 \times 10^5$ cm^{-3}.

Therefore, the fraction (n_{ehot}/n_e) of hot electrons near the wall would be only $f_{hot} = 1.15 \times 10^{-3}$, versus the recorded value of 2×10^{-2} at the center (table 2), if a flat profile for the electron density across the plasma radius is assumed. Obviously, this is not so in glow discharges [1]. As these hot electrons enter the plasma bulk, they are decelerated by collisions and their kinetic energy is reduced to the average values shown in table 2, i.e. a factor 3.5 times lower than the launching value, hence increasing their local density. Electron–neutral inelastic collisions within the sheath width will produce a cascading effect, with secondary electron generation at energies somewhere between the sheath potential and the bulk electron temperature, adding up to the f_{hot} value.

Although these effects would qualitatively account for the relatively high fraction of hot electrons at the center of the discharge as compared with their density at the sheath, no quantitative comparison can be made with the measured f_{hot} values beyond this point without the development of a full kinetic model, adapted to the geometrical characteristics of our reactor, which is outside the scope of this, basically experimental, work.

Even with this limitation, a simple, two-point model can be applied to the data in order to check for the feasibility of the results obtained in pressure sweeps. The model deals only with relative variations of the parameters, less challenging indeed than reproducing the absolute values.

For a typical beam–plasma interaction model, a Lambert–Beer-type equation can be used, $I(x) = I(0) \cdot \exp(-\alpha x)$, with the parameter α playing the role of the extinction coefficient in optical transmission experiments.

Thus, the attenuation of the hot electrons when they enter the plasma bulk could, in principle, be described by a characteristic, pressure-dependent mean free path, $\lambda(P)$, so that

$$f_{hot}(P, x) = f_{hot(wall)} e^{-x/\lambda(P)}, \qquad (8)$$

where x (cm) would be an average distance from the wall to the location of the probe, set at 15 cm in our reactor.

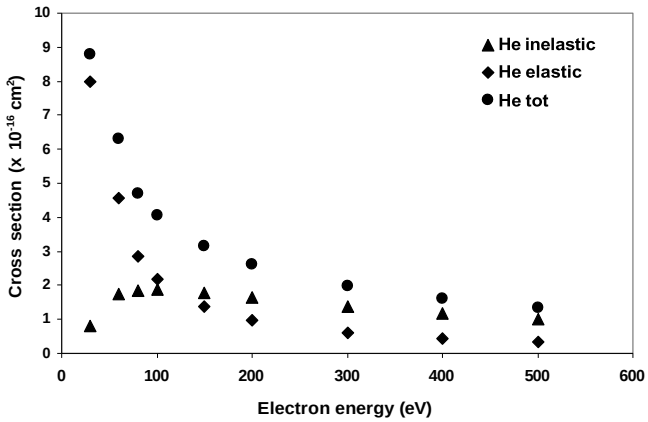

Figure 6. Cross-sections for electron attenuation in He.

If the production of hot secondary electrons by neutral–electron collisions by this fast component of the EEDF can be neglected away from the cathode sheath, then a simple expression for $\lambda(P)$ can be obtained from the kinetic theory:

$$\lambda(P) = v^e/(\sigma v^e)n_{He}, \tag{9}$$

where v^e stands for the velocity of the electrons launched from the cathode (wall) and σ is an effective attenuation cross-section accounting for all processes leading to the scattering and thermalization of these fast electrons. Note that for a monoenergetic distribution of electrons, equation (9) simply becomes $\lambda(P) = 1/(\sigma)n_{He}$ and so equation (8) becomes

$$f_{hot}(P,x) = f_{hot\ wall}\ e^{-x(\sigma)n_{He}}. \tag{10}$$

Ignoring the details about the radial profile developed between the wall and the center of the discharge (corresponding to a simple two-point model), this kind of simple fitting to an exponential can be performed for f_{hot} as well as for T_{hot} from the data displayed in table 2, in order to extract an effective cross-section for the slowing down and thermalization processes within the plasma volume.

Since no measurement of the neutral temperature was available, the conversion factor 1 mTorr $= 3.18 \times 10^{13}$ cm^{-3} at room temperature is used in equation (10), which would underestimate the value of the deduced cross-sections if neutral gas heating takes place within the discharge.

Due to the scarcity of points, only average values for the three current settings can be obtained. From the ln (f_{hot}) and ln (T_{hot}) versus $n_{He}(P)$ behavior of the data shown in table 2, the resulting cross-sections are $\sigma = 2.5 \times 10^{-16}$ cm^2, for f_{hot}, and $\sigma = 1.8 \times 10^{-16}$ cm^2 for T_{hot}, respectively. Both values are in reasonable agreement (taking into account the simplicity of the model) with the bibliographic values displayed in figure 6 for e$^-$ + He inelastic collisions, thus suggesting a negligible role of species other than ground state He in the collisional processes that fast electrons undergo on their way to the sample, as reported under similar plasma conditions in previous works [5, 9, 13, 22, 23].

5. Summary

The existence of a non-negligible suprathermal population in low-pressure He dc glow discharges was addressed. Two different techniques were used for its characterization, providing rather good agreement. This population is only about a few per cent of the total electron content but it can be of significant importance for several processes due to the high energies of these electrons (up to 300 eV). The effective cross-section for the attenuation of these hot electrons deduced from pressure scans is in reasonable agreement with the tabulated values of this parameter corresponding to e + He inelastic collisions in the involved range of energies. Although some simple considerations could account for the small discrepancy between diagnostics, a more complex atomic physics scenario seems to be required for the quantitative interpretation of the reported data on hot tail electron fraction and its average energy.

Acknowledgments

This work was partly supported by the Direccio´n General de Investigacio´n Cient´ıfica y Te´cnica (DGICYT) under Project FIS2010-20911. Also, ABMR and EO were supported by the Madrid Community through the Project TECHNOFUSION (S2009/ENE-1679).

References

[1] Lieberman M A and Lichtenberg A J 1994 *Principles of Plasma Discharges and Materials Processing* (New York: Wiley)
[2] Gill R D, Alper B, Edwards AW, Ingesson L C, Johnson M F and Ward D J 2000 *Nucl. Fusion* **40** 163
[3] Druyvesteyn M J 1930 *Z. Phys.* **64** 781
[4] Matthews G F 1984 *J. Phys. D: Appl. Phys.* **17** 2243
[5] Sugai H, Toyoda H, Nakano K and Isomura N 1995 *Plasma Sources Sci. Technol.* **4** 366
[6] Bran˜as B, Tafalla D, Tabare´s F L and Ortiz P 2001 *Rev. Sci. Instrum.* **72** 602
[7] Oyarzabal E, Mart´ın-Rojo A B, Ferreira J A, Tafalla D and Tabare´s F L 2013 *J. Nucl. Mater.* in press
[8] Blackwell D D and Chen F F 2001 *Plasma Sources Sci. Technol.* **10** 226
[9] Kajita S, Ohno N, Takamura S and Nakano T 2006 *Phys. Plasmas* **13** 013301
[10] Boivin R F, Kline J L and Scime E E 2001 *Phys. Plasmas* **8** 5303
[11] Ralchenko Y 2008 *Atomic Data and Nuclear Data Tables* **94** 603
[12] Chen F F 1965 *Plasma Diagnostic Technics* ed R H Huddlestone and S L Leonard (New York: Academic)
[13] Sugai H, Ghanashev I, Hosokawa M, Mizuno K, Nakamura K, Toyoda H and Yamauchi K 2001 *Plasma Sources Sci. Technol.* **10** 378
[14] Deegan C M, Goss J P, Vender D and Hopkins M B 1999 *Appl. Phys. Lett.* **74** 1969
[15] Mansour ElSabbagh M A, Bowden M D, Uchino K and Muraoka K 2001 *Appl. Phys. Lett.* **78** 3187
[16] Bucvic S and Labat J M 1992 *Phys. Scr.* **46** 57
[17] Tran Ngoc An, Marode E and Johnson P C 1977 *J. Phys. D: Appl. Phys.* **10** 2317

[18] Miura N and Hopwood J 2009 *Rev. Sci. Instrum.* **80** 113502
[19] Knappmiller S, Robertson S and Sternovsky Z 2006 *Phys. Rev.* E **73** 066402
[20] Heer F J and JansenRHJ 1977 *J. Phys. B: At. Mol. Phys.* **10** 18
[21] Medved D B and Strausser Y E 1966 *Adv. Electron. Electron Phys.* **21** 101
[22] Prakash R, Vasu P, Kumar V, Manchanda R, Chodwdhuri M B and Goto M 2005 *J. Appl. Phys.* **97** 043301
[23] Naveed M A, Rehman N U, Zeb S, Hussain S and Zakaullah M 2008 *Eur Phys J.* D **47** 395